Available online at www.sciencedirect.com
SCIENCE DIRECT®
International Journal of Heat and Mass Transfer 48 (2005) 1293–1302
International Journal of HEAT and MASS TRANSFER
www.elsevier.com/locate/ijhmt

Modeling of condensation heat transfer of pure refrigerants in micro-fin tubes

Louay M. Chamra, Pedro J. Mago *, Meng-Onn Tan, Chea-Chun Kung

Department of Mechanical Engineering, Mississippi State University, 210 Carpenter Engineering Building, P.O. Box ME, Mississippi State, MS 39762-5925, USA

Received 15 April 2004; received in revised form 2 October 2004
Available online 8 December 2004

Abstract

A new semi-empirical condensation model for heat transfer coefficient of pure refrigerants flowing inside micro-fin tubes is presented. The new model is developed based on a theoretical analysis of turbulent film condensation inside smooth tubes. Several modifications have been implemented in the original smooth-tube model to account for the heat transfer enhancement effects due to the presence of micro-fins on the internal wall surface. The new condensation model is compared with a set of around 400 experimental data points. The comparison shows that the new model is capable of producing consistent prediction results with a mean absolute deviation less than 20% for most of the available data sets.

Keywords: Condensation; Micro-fin tubes; Heat transfer; Pure refrigerant

1. Introduction

Since the early 1980s the use of micro-fin tubes for commercial and air-conditioning applications has beneficially enhanced the heat transfer performance of tubes with relatively low pressure-drop increases. Micro-fin tubes are found to be one of the most efficient heat transfer enhancement techniques to improve the performance of the heat exchangers. This has been shown by several researchers such as: Cavallini et al. [1], Yu and Koyama [2], and Kedziersky and Goncalves [3]. According to Cavallini et al. [1], micro-fin tubes generally show heat transfer enhancement, with respect to equivalent smooth tubes under the same operating conditions, from 80% to 140% with a pressure-drop increases from 20% to 80%. Similarly, Yu and Koyama [2] showed that the local heat transfer characteristics in a horizontal micro-fin tube are two times higher than those of a smooth tube with the same inner diameter. They attributed the heat transfer enhancement to the enlargement of heat transfer area. Kedziersky and Goncalves [3] presented a local convective-condensation measurement for four refrigerants: R134a, R410A, R125, and R32 in micro-fin tubes. Based on their correlation of the pressure-drop measurements, they suggested that the heat transfer enhancement was due to the fins behaving as a surface roughness.

The presence of the micro-fins on the internal wall surface of the horizontal tubes effectively increases the heat transfer performance of the tubes. This heat transfer enhancement is mainly caused by the helical

* Corresponding author. Tel.: +1 662 325 6602; fax: +1 662 325 7223.
E-mail address: mago@me.msstate.edu (P.J. Mago).

0017-9310/$ - see front matter © 2004 Elsevier Ltd. All rights reserved.
doi:10.1016/j.ijheatmasstransfer.2004.10.005

Nomenclature

c_p	specific heat ($J\,kg^{-1}\,K^{-1}$)
d_i	inner-tube diameter (m)
d_o	outer-tube diameter (m)
$(dp/dz)_f$	frictional pressure gradient ($Pa\,m^{-1}$)
e	micro-fin fin height (m)
f_{LO}	friction factor based on total flow assumed as liquid
f_{GO}	friction factor based on total flow assumed as gas
Fr	Froude number
g	gravitational acceleration ($m\,s^{-2}$)
G	total mass flux ($kg\,m^{-2}\,s^{-1}$)
h	condensation heat transfer coefficient ($W\,m^{-2}\,K^{-1}$)
H	phase change number
k	thermal conductivity ($W\,m^{-1}\,K^{-1}$)
L	heated test section length (m)
$\dot{m}$	mass flow rate ($kg\,s^{-1}$)
MAD	mean absolute deviation
N	total number of data points
n_g	number of micro-fins
p	pressure (Pa)
$P_1 - P_3$	constant defined by Eq. (37)
Pr	Prandtl number (dimensionless)
q	surface heat flux ($W\,m^{-2}$)
Re	Reynolds number
Rx	enhancement factor
Rx_f	empirically-fitted relative roughness
th	tube-wall thickness (without micro-fin) (m)
T	temperature (°C)
T^+	dimensionless temperature
ΔT	wall superheat (°C)
u	velocity ($m\,s^{-1}$)
u^*	friction velocity ($m\,s^{-1}$)
u^+	dimensionless velocity
x	vapor quality
y	distance measured from boundary (m)
y^+	dimensionless distance from the wall
We	Weber number

Greek symbols

β	micro-fin apex angle (degree)
γ	micro-fin helix angle (degree)
μ	dynamic viscosity ($kg\,m^{-1}\,s^{-1}$)
ν	kinematic viscosity ($m^2\,s^{-1}$)
τ	shear stress (Pa)
ε_H	Eddy diffusivity of heat ($m^2\,s^{-1}$)
ε_M	Eddy diffusivity of momentum ($m^2\,s^{-1}$)
α_T	thermal diffusivity
δ	liquid film thickness (m)
δ^+	dimensionless liquid film thickness
Δ	difference
Φ	two-phase multiplier
ρ	density ($kg\,m^{-3}$)
σ	surface tension ($N\,m^{-1}$)

Subscripts

f	frictional
GO	total fluid assumed as vapor
l	liquid-phase only
LO	total fluid assumed as liquid
m	two-phase mixture
sat	saturation
t	turbulent
v	vapor-phase only
w	wall

orientation of the micro-fins that uniformly distribute the liquid film around the circumference of the tube. The transfer enhancement effect is also partly due to an increase in the effective internal wall surface area and to the turbulence induced in the liquid film by the micro-fins.

In the past, many researchers have been involved in determining the performance of the smooth tubes with pure refrigerant as working fluids. Correlations in predicting the condensation heat transfer coefficients for horizontal smooth-tubes have been proposed by the researchers. Generally, these correlations were developed by using empirical methods to compute the condensation heat transfer coefficients. Most of these proposed models are modifications of the Dittus–Boelter single-phase forced convection correlation. Akers et al. [4], Cavallini and Zecchin [5], and Shah [6] presented empirical models that were formulated by using the Dittus–Boelter correlation as a starting point. However, most of these models were developed based on the researchers' own data and are valid only for certain refrigerants. For micro-fin tubes, the available methods for predicting the condensation heat transfer coefficients of tubes were often based on extensions of smooth-tube models. Heat transfer enhancement effect due to the micro-fins have been incorporated by introducing new parameters and generating new empirical constants to the original smooth-tube correlations.

The main objective of the current work is to develop a semi-empirical model for predicting heat transfer coefficients during condensation of pure refrigerants flowing inside different geometries of micro-fin tubes. The validity of the new semi-empirical model is to be evaluated with available experimental data.

Table 1
Flow conditions for pure refrigerants flowing inside micro-fin tubes

Reference	Runs	Fluid	p_{sat} (kPa)	T_{sat} (°C)	q (kW m^{-2})	G (kg m^{-2} s^{-1})	x (mean)
Bogart and Thors [7]	17	R22		40.6		200–800	0.80–0.10
Chamra et al. [8]	24	R22		24		40–200	0.80–0.20
Ebisu and Torikoshi [9]	7	R22		50		85–530	0.80–0.10
Eckels and Pate [10]	20	R134a		30–50		130–420	0.88–0.05
	20	R12					
Eckels et al. [11]	12	R134a	1010	40		80–400	0.88–0.05
Eckels et al. [12]	16	R134a	1010	40		120–400	0.88–0.05
Eckels and Tesene [13]	15	R22		40		100–630	0.95–0.05
	19	R134a					
Goto et al. [14]	52	R22		40		48–598	0.90–0.10
Hitachi Cable [15]	12	R22	1540	40		100–300	0.5
Muzzio et al. [16]	24	R22		35		80–410	0.50
Muzzio et al. [17]	37	R22	1350	35		80–410	0.80–0.10
Schlager [18]	27	R22	1543–1561	40.2–40.7		120–405	0.898–0.092
Schlager et al. [19]	15	R22		39–42		180–550	0.90–0.10
Shinohara and Tobe [20]	9	R22	1400			100–300	0.60
Tang et al. [21]	35	R22		40		250–850	0.50–0.50
		R134a		40		250–750	
Uchida et al. [22]	6	R22		35	2.3–37.2	100–500	0.90–0.10
Yasuda et al. [23]	17	R22		40		100–350	0.60

Table 2
Tube geometries for pure refrigerants flowing inside micro-fin tubes

Reference	Tube material	d_o (mm)	th (mm)	e (mm)	n_g	γ (°)	β (°)	L (m)
Bogart and Thors [7]	Copper	9.53	0.33	0.203	60	18	50	3.66
Chamra et al. [8]	Copper	15.88	0.5	0.35	74–80	15–27	30	2.44
Ebisu and Torikoshi [9]	Copper	7.0	0.3	0.18	50	18	40	3.0
Eckels and Pate [10]	Copper	9.52	0.40	0.20	60	15	50	3.67
Eckels et al. [11]	Copper	9.52	0.30	0.2	60	18	50	3.66
		12.70	0.40	0.2	60	17	50	3.66
Eckels et al. [12]	Copper	9.52	0.30	0.20	60	17	50	3.66
Eckels and Tesene [13]	Copper	9.53	0.305	0.203	60	18	51	3.78
		15.88	0.635	0.305	60	27	45	3.81
		7.94	0.3	0.203	50	18	57	3.78
Goto et al. [14]	Copper	9.52	0.27	0.17	60	25	50	1.0
		6.35	0.27	0.14	55	16		
Hitachi Cable [15]	Copper	9.50–9.52	0.28	0.2–0.21	60	17	40–53	0.50
			0.29			18		
Muzzio et al. [16]	Copper	9.52	0.3	0.15–0.23	54–65	18	40–90	2.6
			0.34			25		
Muzzio et al. [17]	Copper	9.52	0.30	0.195	54	18	40	2.24
Schlager [18]	Copper	9.52	0.40	0.2	60	18	50	3.67
			0.50	0.38	21	30	10	
Schlager et al. [19]	Copper	9.52	0.30	0.2–0.15	60	18–25	40	3.67
Shinohara and Tobe [20]	Copper	9.52	0.30	0.12–0.20	60	7–25	35	0.50
					65		50	
							90	
Tang et al. [21]	Copper	9.52	0.36	0.2	60	0	15	2.83
					72	18	40	
Uchida et al. [22]	Copper	7.0	0.30	0.163	60	18	40	1.09
Yasuda et al. [23]	Copper	9.52	0.30	0.2–0.25	60	18	40	3.05
		7.94			50	30		

2. Experimental database

A database was created from the available experimental data of pure refrigerants flowing inside micro-fin tubes. These data were collected from published papers to help to develop the new pure-refrigerant model and test the validity of the new pure-refrigerant model. Tables 1 and 2 present the pure refrigerants experimental data for flow inside micro-fin tubes. Table 1 lists the flow conditions (saturation pressure, saturation temperature, heat flux, mass flux, and mean vapor quality) and Table 2 delineates the tube geometries (outer tube diameter, minimum wall thickness, fin height, number of fins, helix angle, apex angle, and the heated test section length).

All the experimental data were presented at constant vapor quality with varying mass flux. The mean absolute deviation (MAD) is set as the criterion to determine the effectiveness of a heat transfer model. MAD is defined as the average of the normalized difference between the predicted heat transfer coefficient and the experimental heat transfer coefficient.

$$\mathrm{MAD} = \frac{1}{N}\cdot\sum \frac{|\, h_{\mathrm{experimental}} - h_{\mathrm{predicted}} \,|}{h_{\mathrm{experimental}}} \tag{1}$$

The heat transfer model is considered acceptable if the MAD is less than 30%.

3. New pure-refrigerant model

A new pure-refrigerant model is developed based on a theoretical analysis of turbulent film condensation inside smooth tubes. The flow is assumed to be in the annular regime over the length of the tube. In order to determine the condensation heat transfer coefficient for the turbulent liquid film, the transport of heat in the film, neglecting downstream convection compared to cross-stream diffusion, is given by

$$q = -\left(k + \rho c_p \varepsilon_{\mathrm{H}}\right)\frac{\mathrm{d}T}{\mathrm{d}y} \tag{2}$$

where ϵ_{H} is the turbulent eddy conductivity. By substituting the thermal diffusivity, Eq. (2) becomes

$$q = -\rho c_p(\alpha_{\mathrm{T}} + \varepsilon_{\mathrm{H}})\frac{\mathrm{d}T}{\mathrm{d}y} \Rightarrow q = -\rho c_p \nu\left(\frac{1}{Pr} + \frac{\varepsilon_{\mathrm{H}}}{\nu}\right)\frac{\mathrm{d}T}{\mathrm{d}y} \tag{3}$$

where α_{T} is the thermal diffusivity and Pr is the Prandtl number. Eq. (3) can be expressed in dimensionless form as

$$\frac{q}{q_{\mathrm{w}}} = \left(\frac{1}{Pr} + \frac{\varepsilon_{\mathrm{H}}}{\nu}\right)\frac{\mathrm{d}T^+}{\mathrm{d}y^+} \tag{4}$$

where

$$y^+ = y\frac{u^*}{\nu} \quad \text{with} \quad u^* = \sqrt{\frac{\tau_{\mathrm{w}}}{\rho}} = \sqrt{g\delta} \tag{5}$$

$$T^+ = \frac{\rho c_p u^*}{q_{\mathrm{w}}}(T_{\mathrm{w}} - T) \tag{6}$$

If the turbulent Prandtl number, Pr_{t}, is equal to one, then

$$Pr_{\mathrm{t}} = \frac{\varepsilon_{\mathrm{M}}}{\varepsilon_{\mathrm{H}}} = 1 \Rightarrow \varepsilon_{\mathrm{M}} = \varepsilon_{\mathrm{H}} \tag{7}$$

where ε_{M} is the turbulent eddy diffusivity. Eq. (4) becomes

$$\frac{q}{q_{\mathrm{w}}} = \left(\frac{1}{Pr} + \frac{\varepsilon_{\mathrm{M}}}{\nu}\right)\frac{\mathrm{d}T^+}{\mathrm{d}y^+} \tag{8}$$

Eq. (8) can be integrated from zero to δ^+, where δ^+ is the dimensionless liquid film thickness,

$$\delta^+ = \frac{\delta u^*}{\nu} \tag{9}$$

at $y = \delta^+, T = T_{\mathrm{sat}}$ and at the surface, $y = 0$, $T = T_{\mathrm{w}}$

Therefore,

$$\frac{T_{\mathrm{sat}} - T_{\mathrm{w}}}{(q_{\mathrm{w}}/\rho c_p u^*)} = \int_0^{\delta^+} \frac{\mathrm{d}y^+}{Pr^{-1} + (\varepsilon_{\mathrm{M}}/\nu)}. \tag{10}$$

Eq. (10) can be integrated if the relationship between $\varepsilon_{\mathrm{M}}/\nu$ and y^+ is known. This relationship is established by using the universal velocity distribution expressions

$$\tau = (\mu + \rho\varepsilon_{\mathrm{M}})\frac{\mathrm{d}u}{\mathrm{d}y} \Rightarrow \frac{\tau}{\tau_{\mathrm{w}}} = \left(1 + \frac{\varepsilon_{\mathrm{M}}}{\nu}\right)\frac{\mathrm{d}u^+}{\mathrm{d}y^+} \tag{11}$$

Therefore,

$$1 + \frac{\varepsilon_{\mathrm{M}}}{\nu} = \frac{\tau/\tau_{\mathrm{w}}}{\mathrm{d}u^+/\mathrm{d}y^+} \Rightarrow \frac{\varepsilon_{\mathrm{M}}}{\nu} = \frac{1}{\frac{\mathrm{d}u^+}{\mathrm{d}y^+}} - 1 \tag{12}$$

The von Karman velocity distribution can be used to evaluate $\varepsilon_{\mathrm{M}}/\nu$.

$$y^+ \leqslant 5 \Rightarrow u^+ = y^+ \Rightarrow \frac{\varepsilon_{\mathrm{M}}}{\nu} = 0 \quad \text{Viscous sublayer} \tag{13a}$$

$$5 \leqslant y^+ \leqslant 30 \Rightarrow u^+ = -3.05 + 5\ln(y^+) \Rightarrow \frac{\varepsilon_{\mathrm{M}}}{\nu} = 0.2y^+ - 1 \quad \text{Buffer sublayer} \tag{13b}$$

$$y^+ > 30 \Rightarrow u^+ = 5.5 + 2.5\ln(y^+) \Rightarrow \frac{\varepsilon_{\mathrm{M}}}{\nu} = 0.4y^+ - 1 \quad \text{Turbulent region} \tag{13c}$$

where $u^+ = \frac{\bar{u}}{u^*}$.

Eq. (10) can now be integrated to evaluate the condensation heat transfer coefficient,

$$h = \frac{q}{T_{sat} - T_w} \Rightarrow \frac{\rho c_p u^*}{h} = T^+ = \underbrace{\int_0^5 \frac{dy^+}{Pr^{-1}}}_{\text{Viscous,sublayer}} + \underbrace{\int_5^{26} \frac{dy^+}{Pr^{-1} + (0.2y^+ - 1)}}_{\text{Buffer,sublayer}} + \underbrace{\int_{26}^{\delta^+} \frac{dy^+}{Pr^{-1} + (0.4y^+ - 1)}}_{\text{Turbulent,region}} \quad (14)$$

The dimensionless temperature, T^+, is defined as

$$T^+ = \delta^+ \cdot Pr_l \quad \delta^+ \leqslant 5 \quad (15)$$

$$T^+ = 5 \cdot \left[Pr_l + \ln\left[1 + Pr_l\left(\frac{\delta^+}{5} - 1\right)\right]\right] \quad 5 < \delta^+ \leqslant 30 \quad (16)$$

$$T^+ = 5 \cdot \left[Pr_l + \ln(1 + 5 \cdot Pr_l) + 0.5 \cdot \ln\left(\frac{\delta^+ - 2.5}{27.5}\right)\right] \quad \delta^+ > 30 \quad (17)$$

The dimensionless condensate film thickness, δ^+, for laminar flow can be found by using the Nusselt [24] correlation,

$$\delta^+ = 0.866 Re_l^{0.5} \quad \text{for } Re_l \leqslant 1600 \quad (18)$$

For turbulent flow, the dimensionless film thickness can be found by using the Ganchev and Musvik [25] empirical correlation,

$$\delta^+ = 0.051 Re_l^{0.87} \quad \text{for } Re_l > 1600 \quad (19)$$

where the liquid-phase Reynolds number, Re_l, is

$$Re_l = \frac{4 \cdot \dot{m}_l}{\pi \cdot d_i \cdot \mu_l} = \frac{G \cdot (1 - x) \cdot d_i}{\mu_l} \quad (20)$$

The original model is used to predict the heat transfer coefficient during condensation inside smooth tubes.

$$h = \frac{\rho_l \cdot c_{pl} \cdot \left(\frac{\tau_w}{\rho_l}\right)^{0.5}}{T^+} \quad (21)$$

The frictional component of the two-phase flow pressure gradient $(dp/dz)_f$ is related to the wall shear stress, τ_w, as

$$\pi d \tau_w = \left(\frac{dp}{dz}\right)_f \cdot \frac{\pi d_i^2}{4} \Rightarrow \tau_w = \left(\frac{dp}{dz}\right)_f \cdot \frac{d_i}{4} \quad (22)$$

$(dp/dz)_f$ is defined as the frictional pressure gradient. The value of the frictional pressure gradient is calculated by using the following equations:

$$\left(\frac{dp}{dz}\right)_f = \Phi_{LO}^2 \cdot \left(\frac{dp_f}{dz}\right)_{LO} = \frac{\Phi_{LO}^2 \cdot 2 \cdot f_{LO} \cdot G^2}{d_i \cdot \rho_l} \quad (23)$$

where Φ_{LO} is the two-phase multiplier and f_{LO} is the single-phase friction multiplier. The two-phase multiplier is evaluated by using Friedel [26] correlations.

$$\Phi_{LO} = \sqrt{(1-x)^2 + x^2 \cdot \frac{(\rho_l \cdot f_{GO})}{(\rho_v \cdot f_{LO})} + \frac{3.24 \cdot x^{0.78} \cdot (1-x)^{0.224} \cdot H}{Fr^{0.045} \cdot We^{0.035}}} \quad (24)$$

where Fr is the Froude number, We is the Weber number, H is the phase change number, and f_{GO} and f_{LO} are the smooth tube single-phase friction factors. The Froude, Weber, and phase change numbers can be determined by Eqs. (25)–(27), respectively.

$$H = \left(\frac{\rho_l}{\rho_v}\right)^{0.91} \cdot \left(\frac{\mu_v}{\mu_l}\right)^{0.19} \cdot \left(1 - \frac{\mu_v}{\mu_l}\right)^{0.7} \quad (25)$$

$$We = \frac{G^2 \cdot d_i}{\rho_m \cdot \sigma} \quad (26)$$

$$Fr = \frac{G^2}{g \cdot d_i \cdot \rho_m^2} \quad (27)$$

$$\rho_m = \left(\frac{x}{\rho_v} + \frac{(1-x)}{\rho_l}\right)^{-1} \quad (28)$$

The single-phase friction factors, f_{GO} and f_{LO}, are used in the calculation of the frictional pressure gradient. For micro-fin tubes, Cavallini et al. [1] suggested that the single-phase friction factor to be taken as the higher value of that obtained from the Blasius equation for smooth tubes and that estimated from the Moody diagram under fully-developed turbulent flow and at a relative roughness (empirically fitted). The method is applied to compute the friction factors as

$$f_{LO} = \max(f_{LO1}, f_{LO2}) \qquad f_{GO} = \max(f_{GO1}, f_{GO2})$$

Using the Blasius equation for the turbulent flow

$$f_{LO1} = 0.079 \cdot \left(\frac{G \cdot d_i}{\mu_l}\right)^{-0.25}$$
$$f_{GO1} = 0.079 \cdot \left(\frac{G \cdot d_i}{\mu_v}\right)^{-0.25} \quad \text{when } \frac{G \cdot d_i}{\mu_v} > 2000 \quad (29)$$

and for laminar flow

$$f_{LO1} = \frac{16}{\left(\frac{G \cdot d_i}{\mu_l}\right)} \quad f_{GO1} = \frac{16}{\left(\frac{G \cdot d_i}{\mu_v}\right)} \quad \text{when } \frac{G \cdot d_i}{\mu_v} \leqslant 2000 \quad (30)$$

or for both laminar and turbulent flow, Cavallini et al. [1] proposed the following relations:

$$f_{LO2} = \frac{[1.74 - 2 \cdot \log(2 \cdot Rx_f)]^{-2}}{4} \quad (31)$$

Table 3
Pure-refrigerant data sets used for generating the new empirical constants

Reference	Refrigerant	Number of data points
Hitachi Cable [15]	R22	12
Muzzio et al. [16]	R22	24
Schlager et al. [19]	R22	15
Shinohara and Tobe [20]	R22	9
Tang et al. [21]	R22	35
Yasuda et al. [23]	R22	17
Eckels et al. [11]	R134a	12
Tang et al. [21]	R134a	30
Eckels and Pate [10]	R12	20

Table 4
Mean absolute deviation (MAD) achieved by the new pure-refrigerant model for the data sets used in generating the new empirical constants

Reference	Refrigerant	MAD value (%)
Hitachi Cable [15]	R22	9.9
Muzzio et al. [16]	R22	10.7
Schlager et al. [19]	R22	17.9
Shinohara and Tobe [20]	R22	18.4
Tang et al. [21]	R22	5.6
Yasuda et al. [23]	R22	4.8
Eckels et al. [11]	R134a	14.8
Tang et al. [21]	R134a	5.4
Eckels and Pate [10]	R12	12.7

$$f_{GO2} = \frac{[1.74 - 2 \cdot \log(2 \cdot Rx_f)]^{-2}}{4} \tag{32}$$

where Rx_f is an empirically-fitted relative roughness that is used to model micro-fin tubes and it can be expressed as [1]

$$Rx_f = \frac{0.18 \cdot \left(\frac{e}{d_i}\right)}{(0.1 + \cos\beta)} \tag{33}$$

In order to expand the original smooth-tube model to the micro-fin tubes, a new geometry-enhancement factor, which was introduced by Hori and Shinohara [27], is used. The geometry-enhancement factor, Rx, which accounts for the effects of the heat transfer area increase and the spiral angle, is

$$Rx = \left[\frac{2 \cdot e \cdot n_g \cdot \left(1 - \sin\left(\frac{\beta}{2}\right)\right)}{\pi \cdot d_i \cdot \cos\left(\frac{\beta}{2}\right)} + 1\right] \cdot \frac{1}{\cos(\gamma)} \tag{34}$$

A new correlation to predict the heat transfer coefficient during condensation inside smooth tubes is obtained multiplying Eq. (21) by the enhancement factor for micro-fin tubes, and introducing three empirical constants (P_1,P_2, and P_3), which are generated from the available experimental database. This correlation is given by

$$h = \frac{P_1 \cdot \rho_l \cdot c_{pl} \cdot \left(\frac{\tau_w}{\rho_l}\right)^{P_2}}{T^+} \cdot Rx^{P_3} \tag{35}$$

where τ_w is the wall shear stress.

The MathCad minimize function [28] is used to evaluate the three empirical constants presented in Eq. (35). The new empirical constants for the new pure-refrigerant model were determined using 174 data points collected from seven different sources listed in Table 3. This yields values of $P_1 = 0.208$, $P_2 = 0.224$, and $P_3 = 1.321$.

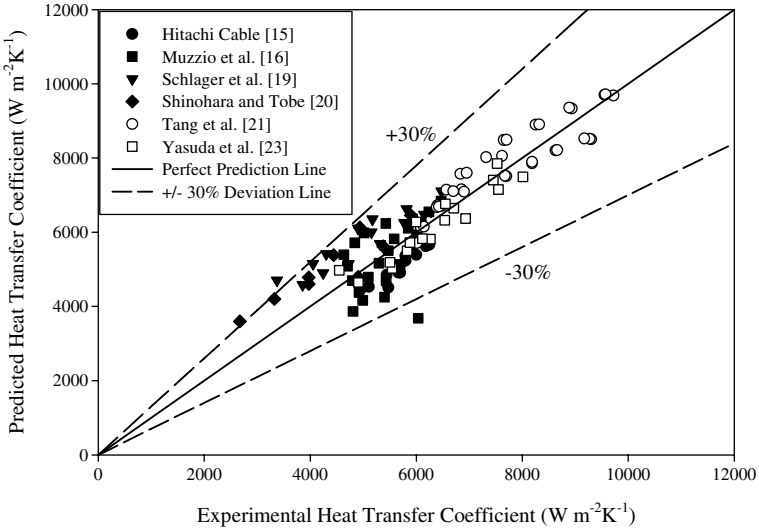

Fig. 1. New model predictions for the R22 data sets used in generating the new empirical constants.

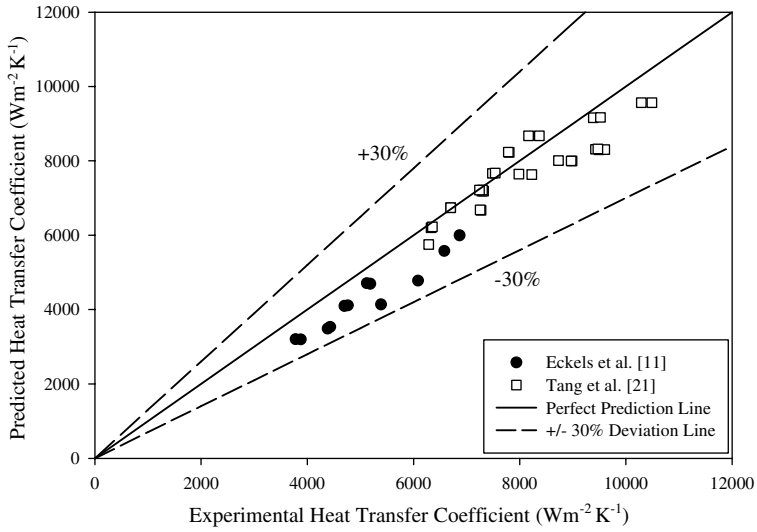

Fig. 2. New model predictions for the R134a data sets used in generating the new empirical constants.

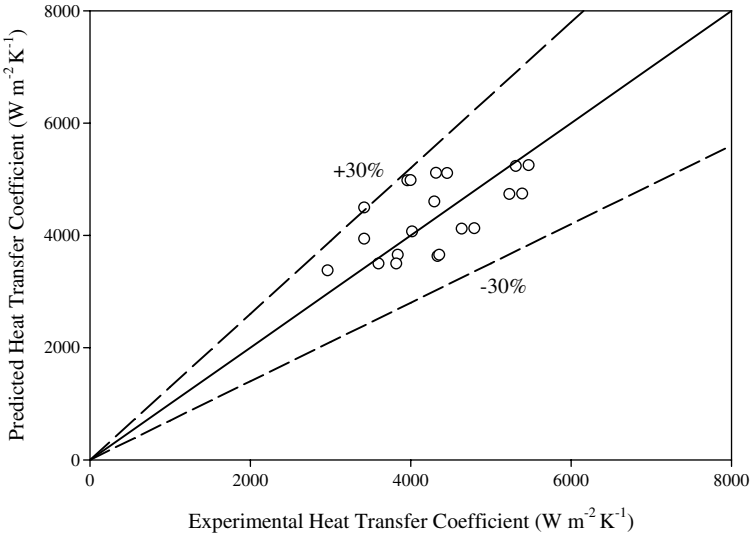

Fig. 3. New pure-refrigerant model prediction for the Eckels and Pate [10] R12 data set.

Introducing the values of the empirical constants into Eq. (35) the final expression to compute the heat transfer coefficient for pure-refrigerant during condensation inside micro-fin tubes can be expressed as

$$h = \frac{0.208 \cdot \rho_l \cdot c_{pl} \cdot \left(\frac{\tau_w}{\rho_l}\right)^{0.224}}{T^+} \cdot Rx^{1.321} \tag{36}$$

where the heat transfer coefficient is in $\mathrm{W\,m^{-2}\,K^{-1}}$.

The new pure-refrigerant model is used to predict existing experimental data and the mean absolute deviation (MAD) value is calculated. For pure refrigerants, the available experimental data have been used to validate the prediction results of the new pure-refrigerant model. The accuracy of the new model in predicting the pure-refrigerant data is presented in Table 4.

Table 4 shows that the prediction results using the new model are excellent since the mean absolute deviations for all these pure-refrigerant data sets are less than 19%. In addition, the new model produces more reliable and consistent prediction results. The prediction results for the nine data sets are illustrated in Figs. 1–3.

The new pure-refrigerant model is further tested with data sets not included in developing the model. The

Table 5
Mean absolute deviation (MAD) achieved by the new pure-refrigerant model on the pure-refrigerant data sets

No.	Reference	Refrigerant	MAD value (%)
1	Bogart and Thors [7]	R22	13.7
2	Chamra et al. [8]	R22	7.7
3	Ebisu and Torikoshi [9]	R22	12.6
4	Eckels and Pate [10]	R134a	12.6
5	Eckels et al. [11]	R134a	18.1
6	Eckels and Tesene [13]	R22	16.5
		R134a	19.1
7	Goto et al. [14]	R22	29.2
8	Muzzio et al. [17]	R22	6.8
9	Schlager [18]	R22	11.9
10	Uchida et al. [22]	R22	22.9

validation process is important to prove the capability of the new model in accurately predicting condensation heat transfer coefficients in micro-fin tubes.

4. Comparison with other experimental data

Additional pure-refrigerant experimental data sets were collected and compared with the prediction results of the new condensation model. These data sets were not included in developing the new model. The capability of the new model to predict the experimental data from other data sets is evaluated. The flow conditions and the tube geometries of the experimental data points are listed in Tables 1 and 2. The prediction results of the new pure-refrigerant model for the experimental data points are shown in Table 5.

A total number of 250 new experimental data points were collected from 10 different sources. These new experimental data were compared with the prediction results from the new pure-refrigerant model. The MAD values are within 20% for most of the experimental data points. This shows that the new pure-refrigerant model is capable of accurately predicting the experimental data points. The prediction results of the new pure-refrigerant model on the additional experimental data sets are shown in Figs. 4 and 5. The prediction results for the Goto et al. [14] R22 data set of the new pure-refrigerant model are relatively high because the experiment is run using a short length of micro-fin tube with low mass flux. The flow configuration inside the Goto et al. [14] experiment may not be in the annular flow regions. Thus, the new pure-refrigerant model, which is applicable only for annular flow regime, achieves high mean absolute deviation for this particular data set.

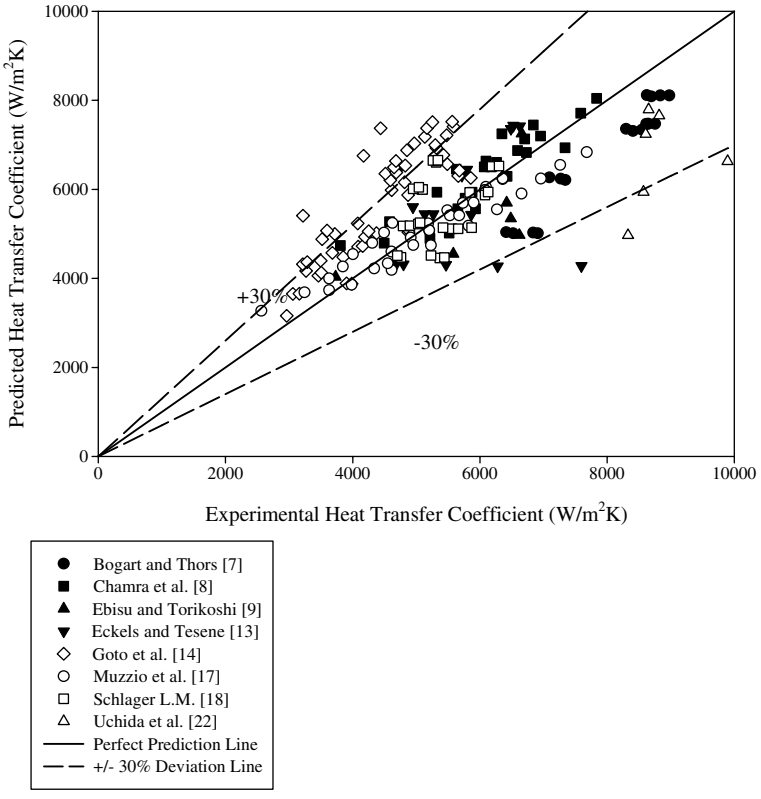

Fig. 4. New model prediction for the new R22 data sets.

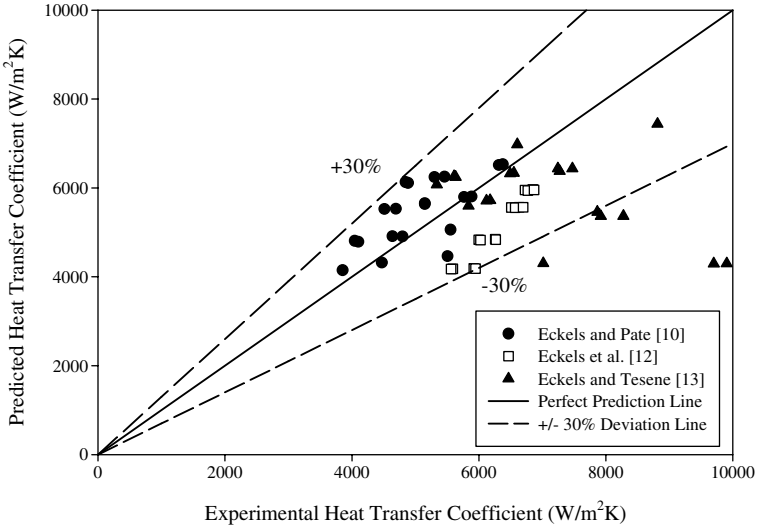

Fig. 5. New model prediction on the new R134a data sets.

Table 6
Comparison of the mean absolute deviation (MAD) of different models for the pure-refrigerant data sets

Reference	Refrigerant	MAD value (%)			
		New pure model	Cavallini et al. [1] model	Yu and Koyama [2] model	Kedzierski and Goncalves [3] model
Eckels and Pate [10]	R134a	12.6	21.5	22.4	12.0
	R12	12.7	16.9	25.1	17.7
Muzzio et al. [16]	R22	10.7	10.3	11.0	20.6
Muzzio et al. [17]	R22	6.8	7.7	15.2	21.7
Schlager [18]	R22	11.9	10.7	38.9	12.6
Schlager et al. [19]	R22	16.6	21.4	44.3	7.8
Shinohara and Tobe [20]	R22	18.4	30.7	166.8	65.6
Tang et al. [21]	R22	5.6	13.8	9.7	26.2
	R134a	5.4	12.2	7.8	22.9
Yasuda et al. [23]	R22	4.8	6.4	16.1	13.2

Table 6 presents a comparison of the mean absolute deviations of the new pure-refrigerant model, the Cavallini et al. [1] model, the Yu and Koyama [2], and the Kedzierski and Goncalves [3] model with the pure-refrigerant data sets. As can be seen, the new pure-refrigerant model MAD values are within 20% for most of the experimental data points. It can also be observed that in most cases the MAD values for the new pure-refrigerant model are lower than those obtained using the Cavallini et al. [1] model, the Yu and Koyama [2] model, and Kedzierski and Goncalves [3] model.

5. Conclusions

A new semi-empirical model for heat transfer coefficient calculation during condensation of pure refrigerants inside micro-fin tubes is presented. The theoretical bases of turbulent film condensation are applied as the fundamental approach to develop the new pure-refrigerant model. The new pure-refrigerant model is validated with the other experimental data that are not used in developing the model. Around 400 experimental data points are used to evaluate the validity of the new pure-refrigerant model. The new pure-refrigerant model is capable of producing consistent prediction results with lower MAD values for most of the available data sets as compares to the other models.

Acknowledgments

The authors would like to express their thanks to Heatcraft Inc. and Wolverine Tube, Inc. for supporting this research and for providing valuable contributions.

References

[1] A. Cavallini, D. Del Col, L. Doretti, G.A. Longo, L.A. Rossetto, A new computational procedure for heat transfer and pressure drop during refrigerant condensation inside enhanced tubes, Enhanced Heat Transfer 6 (1999) 441–456.

[2] J. Yu, S. Koyama, Condensation heat transfer of pure refrigerants in microfin tubes, Proceedings of the 1998 International Refrigeration Conference, Purdue University, 1998, pp. 325–330.

[3] M.A. Kedzierski, J.M. Goncalves, Horizontal convective condensation of alternative refrigerants within a microfin tubes, Enhanced Heat Transfer 6 (1999) 161–178.

[4] W.W. Akers, H.A. Deans, O.K. Crosser, Condensation heat transfer within horizontal tubes, Chemical Engineering Progress Symposium Series 55 (29) (1959) 171–176.

[5] A. Cavallini, R.A. Zecchin, A dimensionless correlation for heat transfer in forced convection condensation, Proceedings of the Sixth International Heat Transfer Conference 3 (1974) 309–313.

[6] M.M. Shah, A general correlation for heat transfer during film condensation inside pipes, International Journal of Heat and Mass Transfer 22 (4) (1979) 547–556.

[7] J. Bogart, P. Thors, In-tube evaporation and condensation of R-22 and R-410A with plain and internally enhanced tubes, Enhanced Heat Transfer 6 (1999) 37–50.

[8] L. Chamra, R.L. Webb, M.R. Randlett, Advanced microfin tubes for condensation, International Journal of Heat and Mass Transfer 39 (9) (1996) 1839–1846.

[9] T. Ebisu, K. Torikoshi, In-tube heat transfer characteristics of refrigerant mixtures of HFC-32/134a and HFC-32/125/134a, International Refrigeration Conference, Purdue University, 1994, pp. 293–298.

[10] S.J. Eckels, M.B. Pate, Evaporation and condensation of HFC-134a and CFC-12 in a smooth tube and a micro-fin tube, ASHRAE Transactions 97 (2) (1991) 71–81.

[11] S.J. Eckels, T.M. Doerr, M.B. Pate, Heat transfer coefficients and pressure drops for R-134a and an ester lubricant mixture in a smooth tube and a micro-fin tube, ASHRAE Transactions 104 (1a) (1998) 366–375.

[12] S.J. Eckels, T.M. Doerr, M.B. Pate, A comparison of the heat transfer and pressure drop performance of R134a-lubricant mixtures in different diameter smooth tubes and micro-fin tubes, ASHRAE Transactions 104 (1a) (1998) 376–386.

[13] S.J. Eckels, B.A. Tesene, A comparison of R22, R134a, R410a, and R407c condensation performance in smooth and enhanced tubes: Part I, Heat transfer, ASHRAE Transaction 105 (1999) 428–441.

[14] M. Goto, N. Inoue, K. Koyama, Condensation heat transfer of HFC-22 and its alternative refrigerants inside an internally grooved horizontal tube, Proceedings of 19th International Congress on Refrigeration, The Hagul, 1995, pp. 254–260.

[15] Hitachi Cable, Ltd., Technical Data 14-958, Effect on performance of expanding the thermofin-EX and thermofin-HEX, tube; Hitachi Cable, Ltd. (1987) 14–958.

[16] A. Muzzio, A. Niro, S. Arosio, Heat transfer and pressure-drop during evaporation and condensation of R22 inside 9.52-mm O.D. micro-fin tubes of different geometries, ASHRAE Transactions 101 (1) (1995) 1055–1061.

[17] A. Muzzio, A. Niro, S. Arosio, Heat transfer and pressure drop during evaporation and condensation of R22 inside 9.52-mm O.D. microfin tubes of different geometries, Enhanced Heat Transfer 5 (1) (1998) 39–52.

[18] L.M. Schlager, The effect of oil on heat transfer and pressure drop during evaporation and condensation of refrigerant inside augmented tubes, Ph.D. Thesis, Iowa State University, Ames, Iowa, 1988.

[19] L.M. Schlager, M.B. Pate, A.E. Bergles, Heat transfer and pressure drop during evaporation and condensation of R22 in horizontal micro-fin tubes, International Journal of Refrigeration 12 (1989) 6–14.

[20] Y. Shinohara, M. Tobe, Development of an improved "Thermofin Tube", Hitachi Cable Review 4 (1985) 47–50.

[21] L.Y. Tang, M.M. Ohadi, A. Johnson, Flow condensation in smooth and micro-fin tubes with HFC-22, HFC-134a and HFC-410A refrigerants Part I: experimental results, Enhanced Heat Transfer 7 (2000) 289–310.

[22] M. Uchida, M. Itoh, N. Shikazono, M. Kudoh, Experimental study on the heat transfer performance of a zeotropic refrigerant mixture in horizontal tubes. Proceedings of the 1996 International Refrigeration Conference, University of Purdue, 1996, pp. 133–138.

[23] K. Yasuda, K. Ohizumi, H. Makoto, O. Kawamata, Development of condensing "Thermofin-Hex-C Tube", Hitachi Cable Review 9 (1990) 27–30.

[24] W. Nusselt, Die Oberflachenkondensation des wasserdampfes, Zeitsch. Ver. Deutsch. Ing. 60 (1916) 541, and 569.

[25] B.G. Ganchev, A.B. Musvik, Experimental study of hydrodynamic and heat-transfer processes in the downward motion of a two-phase flow under annular and dispersed-annular conditions, Journal of Engineering Physics 31 (1) (1976) 760–766.

[26] L. Friedel, Improved friction pressure drop correlations for horizontal and vertical two phase pipe flow, paper E2, European Two Phase Flow Group Meeting, Ispra, Italy, 1979.

[27] M. Hori, H. Shinohara, Internal heat transfer characteristics of small-diameter thermofin tubes, Hitachi Cable Review 10 (1991) 85–90.

[28] MathCAD 2000 Professional, Mathsoft Inc, Cambridge, MA, 1995.